



# Characterization of a quorum sensing device for synthetic biology design: Experimental and modeling validation



Nazanin Saeidi, Mohamed Arshath, Matthew Wook Chang, Chueh Loo Poh \*

School of Chemical and Biomedical Engineering, Nanyang Technological University, Singapore 637459, Singapore

## HIGHLIGHTS

- ▶ We developed mathematical model that simulates dynamic and static performance of a biological device.
- ▶ We modeled an example quorum sensing device that produces GFP in the presence of AHL.
- ▶ Simulation results show that the model was able to simulate behavior similar to experimental results.
- ▶ Standard SBML (system biology markup language) format was used to store the model.
- ▶ The model follows the MIRIAM and MIASE compliances.

## ARTICLE INFO

### Article history:

Received 10 September 2012

Received in revised form

30 November 2012

Accepted 7 December 2012

Available online 22 December 2012

### Keywords:

Synthetic biology

Mathematical modeling

Simulation

Biological engineering

Computer aided design

Quorum Sensing

## ABSTRACT

Modeling of biological parts is of crucial importance as it enables the *in silico* study of synthetic biological systems prior to the actual construction of genetic circuits, which can be time consuming and costly. Because standard biological parts are utilized to build the synthetic systems, it is important that each of these standard parts is well characterized and has a corresponding mathematical model that could simulate the characteristics of the part. These models could be used in computer aided design (CAD) tools during the design stage to facilitate the building of the model of biological systems. This paper describes the development of a mathematical model that is able to simulate both the dynamic and static performance of a biological device created using standard parts. We modeled an example quorum sensing device that produces green fluorescent protein (GFP) as reporter in the presence of Acyl Homoserine Lactone (AHL). The parameters of the model were estimated using experimental results. The simulation results show that the model was able to simulate behavior similar to experimental results. Since it is important that these models and the content in the models can be searchable and readable by machines, standard SBML (system biology markup language) format was used to store the models. All parts and reactions are fully annotated to enable easy searching, and the models follow the Minimum Information Requested In the Annotation of Models (MIRIAM) compliance as well as the Minimum Information About a Simulation Experiment (MIASE).

© 2012 Elsevier Ltd. All rights reserved.

## 1. Introduction

Synthetic biology involves engineering biological systems with novel functions by using standard, reusable, interchangeable biological parts. The use of these standard biological parts enables the utilization of engineering principles such as standardization, decoupling, and abstraction for more efficient engineering of biological systems (Endy, 2005). Synthetic biology has shown that its framework can be implemented to develop novel biological systems to produce biofuels (Steen et al., 2010), to degrade pollutants in water

(Sinha et al., 2010), to produce drugs (Ro et al., 2006), and to sense and kill a pathogen (Saeidi et al., 2011a, 2011b).

There are now a number of registries of biological parts such as MIT registry of standard biological parts (<http://partsregistry.org/>) and BglBricks (Anderson et al., 2010). These biological parts range from promoters to composite of parts which form devices with more complex functions. In order to provide important and useful information about these parts for the development of new complex biological systems, these parts need to be well characterized. To address the challenge of characterizing standard biological parts, Canton et al. proposed a framework in which both static and dynamic performance of a device were characterized and presented in a form of datasheet for easy reference (Canton, 2008). Static and dynamic performances of devices are important characteristics. Static performance describes the steady

\* Corresponding author. Tel.: +65 6514 1088; fax: +65 6791 1761.  
E-mail address: CLPoh@ntu.edu.sg (C.L. Poh).

state relationship between the input and output of the device while dynamic performance describes the dynamic response of the device to a step increase at time zero. These two characteristics are useful in predicting the output amount and studying the response time of composed systems (Canton, 2008). To enable more efficient design of complex biological systems, it is important that this information about the characteristics of the parts is readily accessible by computer aided design (CAD) tools. Consequently, it has been proposed that each standard biological part should have a corresponding standard model that can provide necessary characteristics about the parts to perform modeling of biological systems *in silico* (Rouilly et al., 2007). Because it is important to have quantitative, reproducible models that can stimulate and reproduce the static and dynamic characteristics of standard biological parts/devices, in this study, we developed a mathematical model that is able to simulate both the dynamic and static performance of a standard biological device and embed information such as rate constants for reactions involved into the model to facilitate integration of different parts into a composed system.

This paper presents the development of the quantitative model that is able to simulate both static and dynamic performance of a biological device. In this work, we modeled a quorum sensing device fused with green fluorescent protein (GFP). This sensing device is able to sense *Pseudomonas aeruginosa* (a human pathogen) based on quorum sensing and was utilized in a larger biological system which is capable of sensing and killing *P. aeruginosa* (Ling, 2010; Saeidi et al., 2011a, 2011b). Experiments were performed for parameters estimation and model validation. As the model should be machine readable and searchable so that the model and its content can be readily accessed by CAD tools, our model is stored using system biology markup language (SBML) with all the entities in the model fully annotated based on MIRAM, the Minimum Information Requested in the Annotation of Models (Novere et al., 2005). To ensure that our model is reproducible and reusable, we adhered to the recently introduced MIASE requirements, the Minimum Information About a Simulation Experiment (Waltemath et al., 2011).

## 2. Materials and methods

### 2.1. Strains and media

All cells involved in cloning and characterization experiments are *E. coli* TOP10 (Invitrogen). Supplemented M9 media (M9 salts,

1 mM thiamine hydrochloride, 0.4% glycerol, 0.2% casamino acids, 0.1 M  $MgSO_4$ , 0.5 M  $CaCl_2$ ) was used as a medium for the characterization. Ampicillin (100  $\mu g/mL$ ) was added to the culture media for antibiotic selection where appropriate. Homoserine lactone (3OC<sub>12</sub>HSL; Sigma Aldrich) was used for characterization experiments. All restriction and ligation enzymes were purchased from New England Biolabs (NEB). Table 1 summarizes all plasmids, biobrick parts and devices used in this study. Genetic mapping of engineered construct is illustrated in the supplementary information of our previous work (Saeidi et al., 2011a, 2011b).









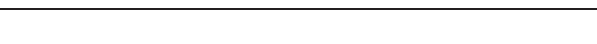
### 2.2. System assembly

The genetic constructs developed in this study were assembled using standard synthetic biology protocols (Shetty, 2008). Briefly, for front insertion of biobrick parts, purified insert and vector plasmids were digested with EcoRI/SpeI and EcoRI/XbaI respectively. For back insertion to upstream vector, the insert and vector plasmids were digested with XbaI/PstI and SpeI/PstI in that order. Digested fragments were separated by DNA gel electrophoresis and ligated with NEB Quick Ligase in accordance with the manufacturer's instructions. Plasmids from chemically transformed cells were purified by affinity columns and verified by DNA sequencing.

### 2.3. Design of the quorum sensing device

The sensing device was designed based on the Type I quorum sensing mechanism of *P. aeruginosa* (Fig. 1). The pTetR is a constitutive promoter. Hence, LasR which is a transcriptional activator will be constitutively produced and bind to 3OC<sub>12</sub>HSL to form LasR-3OC<sub>12</sub>HSL complex. This complex will then bind to the luxR promoter (pLuxR), leading to the production of GFP which serves as a reporter to characterize the steady state and dynamic performance of the quorum sensing device. We have focused on sensitivity to AHL as the key specification of the sensing device. Characterization of the sensing device in our earlier study indicated that *P. aeruginosa* produced 1.0E–7 to 1.0E–6 M of 3OC<sub>12</sub>HSL (Saeidi et al., 2011a, 2011b) and previous studies estimated extracellular concentration of 3OC<sub>12</sub>HSL to be in the range of 1.0E–6 to 1.0E–4 M within proximity to the site of *P. aeruginosa* infection (Charlton et al., 2000; Pearson et al., 1995). Hence, the sensing device needs to be sensitive to the 1.0E–7 to 1.0E–6 M of AHL. The performance of the sensing

**Table 1**  
List of all genetically encoded parts, devices and systems used in this work. The part number, functional description and symbol used are listed for each component. Descriptions of all Bba parts can be found in the MIT Registry of Standard Biological Parts while the rest are explained in text.

Part Number	Description	Symbol
BBa-R0040	TetR repressible promoter	
BBa-R0062	LuxR and AHL inducible promoter	
BBa-B0032	Ribosome binding site (medium)	
BBa-B0034	Ribosome binding site (strong)	
BBa-C0179	LasR coding region	
BBa-E0040	Green fluorescence protein	
BBa-B0015	Terminator	
pTetR-LasR-pLuxR	Sensing device	
pTetR-LasR-pLuxR-GFP	Sensing device with reporter protein	

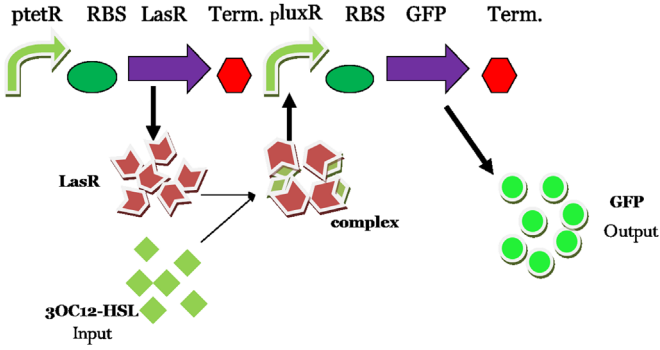


**Fig. 1.** Schematic of the quorum sensing system modeled. The system is based on the type I quorum sensing mechanism of *P. aeruginosa*. The TetR promoter (pTetR), which is constitutively on, produces a transcriptional factor (LasR) that binds to AHL (3OC<sub>12</sub>HSL). The *LuxR* promoter (pLuxR), to which LasR–AHL activator complex binds, serves as the inducible promoter in our sensing system. The formation of the LasR–AHL complex, which binds to the *luxR* promoter, leads to the production of GFP as the reporter protein.

device should be reproducible under same condition. It is worth noting that the current device response time is about 2–3 h.

#### 2.4. Characterization of sensing device (pTetR–LasR–pLuxR–GFP) with 3OC<sub>12</sub>HSL

Single colonies of *E. coli* (Top10) with pTetR–LasR–pLuxR–GFP were each inoculated into 5 mL of prewarmed supplemented M9 ampicillin for overnight culture in a shaking incubator at 37 °C. After overnight growth, the cultures were diluted to OD<sub>600</sub> of 0.02 and allowed to incubate further to OD<sub>600</sub> of 0.5 under the same condition. Cultures were then transferred into a transparent, flat-bottom 96 well plate in triplicate aliquots of 200 µL for induction with 3OC<sub>12</sub>HSL at varying molar concentrations (0, 5E–10, 1E–9, 1E–8, 5E–8, 1E–7, 5E–7, 1E–6, 5E–6, 1E–5, and 1E–4 M). The plate was incubated at 37°C with rapid shaking in a microplate reader (BioTek) and assayed for green fluorescence. Time-series fluorescence and OD<sub>600</sub> data were obtained at intervals of 10 min for a total run time of 5 h. The experiments were done with two biological replicates and three technical replicates. The experimental result was zeroed with supplemented M9 to remove background fluorescence and OD<sub>600</sub>.

We chose these concentrations as our sensing device designed to sense the presence of *P. aeruginosa* (Saeidi et al., 2011a, 2011b). Therefore, for our sensing device to be useful it should be able to detect the native 3OC<sub>12</sub>HSL concentration produced by *P. aeruginosa* as described in Section 2.3.

#### 2.5. Model of the sensing device

The model developed comprises of 6 first order ordinary differential equations (ODEs) which represent the reactions involved and the kinetics of the quorum sensing device. Fig. 1 illustrates the steps involved in triggering the production of reporter protein GFP.

The constitutive production of LasR is described by Eqs. (1) and (2). We assume that LasR mRNA and LasR protein are produced according to the law of mass action at the rate of  $k_1$  and  $k_2$  and are degraded with the rate of  $y_1$  and  $y_2$ , respectively.

$$\frac{d[mRNA_{LasR}]}{dt} = k_1[pTetR] - y_1[mRNA_{LasR}] \quad (1)$$

$$\frac{d[LasR]}{dt} = k_2[mRNA_{LasR}] - y_2[LasR] \quad (2)$$

The rate of complex formation between LasR protein and 3OC<sub>12</sub>HSL (AHL) is represented in Eq. (3) where LasR–AHL denotes the complex. The complex formation rate is directly proportional to the concentration of LasR and AHL present, where  $k_3$  denotes the association rate constant (Fagerlind et al., 2005) and  $k_4$  denotes the dissociation rate.

$$\frac{d[LasR-AHL]}{dt} = k_3[LasR][AHL] - k_4[LasR-AHL] \quad (3)$$

Eq. (4) represents the change in concentration of AHL.

$$\frac{d[AHL]}{dt} = -k_3[LasR][AHL] + k_4[LasR-AHL] \quad (4)$$

Eq. (5) represents the binding of unoccupied pLuxR promoter (pLuxR) to LasR–AHL complex, in which  $k_5$  denotes the association rate,  $k_6$  denotes the dissociation rate and A.pLuxR represents the occupied form of pLuxR (Hooshangi et al., 2005).

$$\frac{d[A.pLuxR]}{dt} = k_5[LasR-AHL][pLuxR] - k_6[A.pLuxR] \quad (5)$$

Eq. (6) describes the production GFP by the active complex (A.pLuxR). We have assumed that AHL concentration is negligible when compared to pLuxR concentration. Furthermore, because we are using PSB1A2 which is a high copy number plasmid (100–300 per cell), considering pluxR in excess is a reasonable assumption. Hence, we considered that A.pluxR concentration mainly depends on the AHL concentration.

$T$  in Eq. (6) denotes the time constant which represents the time it takes for the system response to reach 63.2% of its maximum output.  $GFP_{max}$  is the maximum GFP (amount of GFP at steady state) produced at different AHL concentrations. Because experimental results show that  $1/T$  and  $GFP_{max}$  varied in a Hill equation like manner when AHL concentration increases, two Eqs. (6.1) and (6.2) were introduced to represent the change of  $1/T$  and  $GFP_{max}$  with AHL, respectively. Eqs. (6.1) and (6.2) are functions in terms of the A.pLuxR

$$\frac{d[GFP]}{dt} = \frac{1}{T}(GFP_{max} - [GFP]) \quad (6)$$

$$\frac{1}{T} = k_7 + \frac{k_8[A.pLuxR]^{n_1}}{k_9^{n_1} + [A.pLuxR]^{n_1}} \quad (6.1)$$

$$GFP_{max} = k_{10} + \frac{k_{11}[A.pLuxR]^{n_2}}{k_{12}^{n_2} + [A.pLuxR]^{n_2}} \quad (6.2)$$

#### 2.6. Parameter derivation

Parameters for Eqs. (1)–(5) were obtained or derived from literature. Parameters  $k_1$  and  $k_2$  in Eq. (1) were derived based on information provided in BioNumbers, the database of useful biological numbers. BioNumber ID:104902 (RNA polymerase transcription rate of mRNA in different media and doubling times) was used to calculate  $k_1$  (Vogel and Jensen, 1994). While BioNumber ID:100059 (Rate of translation by ribosome) and distance between ribosome on each mRNA (Bremer, 1996) were used to derive  $k_2$ . Table 2 summarizes the parameters related to Eqs. (1)–(5). To derive the parameters for Eqs. (6), (6.1) and (6.2), experiments in which the quorum sensing device was characterized were performed. Two independent experiments were carried out. Each experiment had two biological replicates and three technical replicates. The data from the first experiment was used to estimate the parameters of Eqs. (6.1) and (6.2) while the data from the second experiment was used to verify the model. Table 4 shows the parameters value of Eqs. (6.1) and (6.2).

In the experiments, time-series fluorescence and OD<sub>600</sub> data were obtained at intervals of 10 min for a total run time of 5 h.

**Table 2**

List of all the parameters for Eqs. (1)–(5), which are taken from literatures.

Parameters	Definition	Value	Reference
$k_1$	Synthesis rate of mRNA (LasR) ( $\text{min}^{-1}$ )	3.734	<a href="http://Bionumbers.harvard.edu">http://Bionumbers.harvard.edu</a> Derived based on BioNumber ID: 104902
$y_1$	mRNA (LasR) decay rate ( $\text{min}^{-1}$ )	0.348	(Elowitz and Leibler, 2000)
$k_2$	Synthesis rate of LasR ( $\text{min}^{-1}$ )	35.7	<a href="http://Bionumbers.harvard.edu">http://Bionumbers.harvard.edu</a> Derived based on BioNumber ID: 100059 and (Bremer, 1996)
$y_2$	Decay rate of LasR ( $\text{min}^{-1}$ )	0.0696	(Basu et al., 2005)
$y_3$	Decay rate of 3OC <sub>12</sub> HSL ( $\text{min}^{-1}$ )	2.83E–4	(Kaufmann et al., 2005)
$k_3$	Association rate of LasR and 3OC <sub>12</sub> HSL ( $\text{M}^{-1}\text{min}^{-1}$ )	9.6E+6	(Fagerlind et al., 2005)
$k_4$	Dissociation rate of LasR and 3OC <sub>12</sub> HSL ( $\text{min}^{-1}$ )	0	Assumption for long chain AHLs
$k_5$	Association rate of LasR-3OC <sub>12</sub> HSL and pLuxR ( $\text{M}^{-1}\text{min}^{-1}$ )	1.98E+6	(Hooshangi et al., 2005) (tuned)
$k_6$	dissociation rate of LasR-3OC <sub>12</sub> HSL and pLuxR ( $\text{min}^{-1}$ )	10.2	(Hooshangi et al., 2005) (tuned)

**Table 3**Derived parameters using 1st set of experiment, to find out  $GFP_{max}$  and  $1/T$ .

AHL concentrations	$GFP_{max}$ (M)	$T$ (min)	$1/T$ ( $\text{min}^{-1}$ )	$R^2$
5.00E–10	7.5E–16	210	0.0048	0.826
1.00E–09	8.5E–16	205	0.0049	0.866
1.00E–08	8.90E–16	190	0.0053	0.904
5.00E–08	1.20E–15	135	0.0074	0.960
1.00E–07	1.90E–15	115	0.0087	0.937
5.00E–07	6.20E–15	90	0.0111	0.953
1.00E–06	9.3E–15	89	0.0112	0.936
5.00E–06	1.03E–14	85	0.0118	0.922

**Table 4**

Parameters after estimated empirically for Eqs. (6.1) and (6.2).

Parameter	Equation	Value
$K_7(1/\text{min})$	(6.1)	0.0041
$K_8(1/\text{min})$	(6.1)	0.0096
$K_9([M])$	(6.1)	9.74E–08
$n_1$	(6.1)	2
$K_{10}([M]/\text{cell})$	(6.2)	6.50E–16
$K_{11}([M]/\text{cell})$	(6.2)	1.00E–14
$K_{12}([M])$	(6.2)	2.40E–07
$n_2$	(6.2)	2

Relative Fluorescence Unit (RFU) which is an indirect way of GFP concentration was then divided by  $OD_{600}$  at each time point. The data were converted to absolute units ( $CFU_{\text{per well}}$  and [GFP] in molar) using Eqs. (7)–(9). These equations were derived by calibrating the BioTek microplate reader, according to the protocol in (Canton, 2008).

$$CFU_{\text{perwell}} = OD_{600} \times 3E+8 \quad (7)$$

$$[GFP] = RFU \times 1.28E-8 \quad (8)$$

$$\frac{[GFP]}{CFU_{\text{perwell}}} \approx \frac{RFU}{OD_{600}} \times 4E-17 \quad (9)$$

To obtain parameters for Eqs. (6.1) and (6.2),  $GFP_{max}$  and  $T$  at different AHL concentrations need to be first derived. This was achieved by fitting Eq. (10) to the curve representing the GFP production over time (dynamic characteristics) for each different AHL concentration. The parameter  $t$  in Eq. (10) refers to the time as the variable and parameter  $T$  denotes the time constant which represents the time it take for the system to reach 63.2% of its maximum output.

$$[GFP] = GFP_{max} \left(1 - e^{-t/T}\right) \quad (10)$$

Parameters in Eqs. (6.1) and (6.2) were then estimated by fitting  $1/T$  at different AHL concentrations and by fitting  $GFP_{max}$  at

different AHL concentrations, respectively. All fitting of curves were performed using cftool in Matlab (Mathworks, Inc, NA). CellDesigner 4.1with SBML ODE solver and Copasi (Funahashi et al., 2003, 2008) was used to construct the model and run the simulation.

## 2.7. Sensitivity analysis assay

To analyze the sensitivity of the various parameters in the model, sensitivity analysis was performed. To carry out the sensitivity analysis, each parameter was varied in range from –80% to +100% (at an interval of 20%) from the original value which was obtained either from literature or from parameter fitting. To compare the sensitivity assay results obtained from simulation, two graphs were drawn: percentage difference in original output value at 300 min versus percentage change in parameter value at AHL concentration of 5E–7 M as the medium input of the quorum sensing device, and percentage change in time to reach steady state versus percentage change in parameter value. We chose this concentration as our sensing device should be able to detect the AHL in the range of 1E–7 to 1E–6. Hence we picked 5E–7 M as the average AHL concentration.

## 2.8. Model validation

To verify the reproducibility of our proposed model, an independent set of experimental results was obtained to compare with the simulation results derived using the proposed model. To validate the simulation results for steady state GFP concentration, simulations with different concentrations of AHL (0, 5E–10, 1E–9, 1E–8, 5E–8, 1E–7, 5E–7, 1E–6, 5E–6, 1E–5, and 1E–4 M) were performed for 100 time steps over 300 min. Furthermore, the ODEs were solved at steady-state to analytically derive the transfer function from AHL to GFP. The steady state value of GFP obtained using the simulation results and analytical transfer function were compared to the experimental results obtained using different concentrations of AHL. To validate the simulation results for dynamic GFP production, simulation was run using the same conditions as before at 3 different AHL input concentrations: low, medium and high input (i.e., 5E–10, 5E–7 and 5E–6 M of AHL, respectively) and simulation results were compared with experimental results under same conditions (e.g. same AHL concentrations and over 300 min).

## 2.9. Format and annotation of the model

To ensure that our model and the content in the model are searchable and readable by machines, standard SBML format was used and all parts and reactions were fully annotated according to MIRIAM. Further, to ensure that the simulation results are reproducible, we adhered to the MIASE requirements.



MIRIAM is a standard for reference correspondence dealing with syntax and semantics of the model and an annotation scheme that specifies the documentation of the model by external knowledge (Noverre et al., 2005). Annotation is composed of two key components. Firstly, it gives an attribution to the entity, covering the absolute minimum information that is required to associate the model with both a reference description and an encoding process. Secondly, it is linked to external data resources. Although the MIRIAM promotes the communication and reusability of quantitative biochemical models, it is not enough for efficient reuse of models in a quantitative setting. Consequently, MIASE which describes the minimal information that must be provided with a simulation experiment for others to use was recently introduced. It is essential to include the core information required to perform the simulation of quantitative models (Waltemath et al., 2011).

### 3. Results

#### 3.1. Characterization of sensing device (pTetR-LasR-pLuxR-GFP) with 3OC<sub>12</sub>HSL

To characterize and evaluate our proposed model of the quorum sensing device, GFP was ligated downstream to the sensing device (i.e. pTetR-LasR-pLuxR-GFP). To obtain the characteristics of the sensing device, GFP concentration over the number of cells in one well was monitored at a range of concentrations of inducer 3OC<sub>12</sub>HSL. The results from two independent experiments were obtained (Fig. 2). In both experiments,

the results show that there was a sharp increase in GFP production as the 3OC<sub>12</sub>HSL concentration increased. This transition occurred at inducer concentration from 0 to 1E–6 M, after which it started to decline. We observed a decline in GFP response at AHL concentration greater than 1E–6. We observed a decline in GFP response at AHL concentration greater than 1E–6. This decline could be due to the over production of GFP and its toxicity to the cells, causing *E. coli* to die. The switch point of the sensing device is at 2.4E–7 M. This shows that the optimum detection range of 3OC<sub>12</sub>HSL for this quorum sensing device is between 1E–7 M and 1E–6 M.

#### 3.2. Parameters derivation

Table 2 summarizes the parameters that were derived from literature. These parameters were used in Eqs. 1–5 of our proposed model. Most of the parameters were extracted directly from the corresponding literature (Basu et al., 2005; Elowitz and Leibler, 2000; Fagerlind et al., 2005; Hooshangi et al., 2005; Kaufmann et al., 2005), except for  $k_1$  and  $k_2$ . These two parameters represent LasR mRNA and LasR protein synthesis rate respectively.  $k_1$  was calculated to be 0.0622 s<sup>–1</sup> or 3.734 min<sup>–1</sup> by considering that the length of LasR mRNA is 723 nucleotides and mRNA chain elongation rate to be 45 residues s<sup>–1</sup> (according to BioNumber ID:104902). For  $k_2$  derivation, by taking into account the length of LasR which is 241 amino acids and translation rate of 16 amino acids s<sup>–1</sup> which is obtained from (BioNumber ID: 100059), rate of a LasR synthesis was calculated to be 16/241=0.07 s<sup>–1</sup>. To calculate the number of active

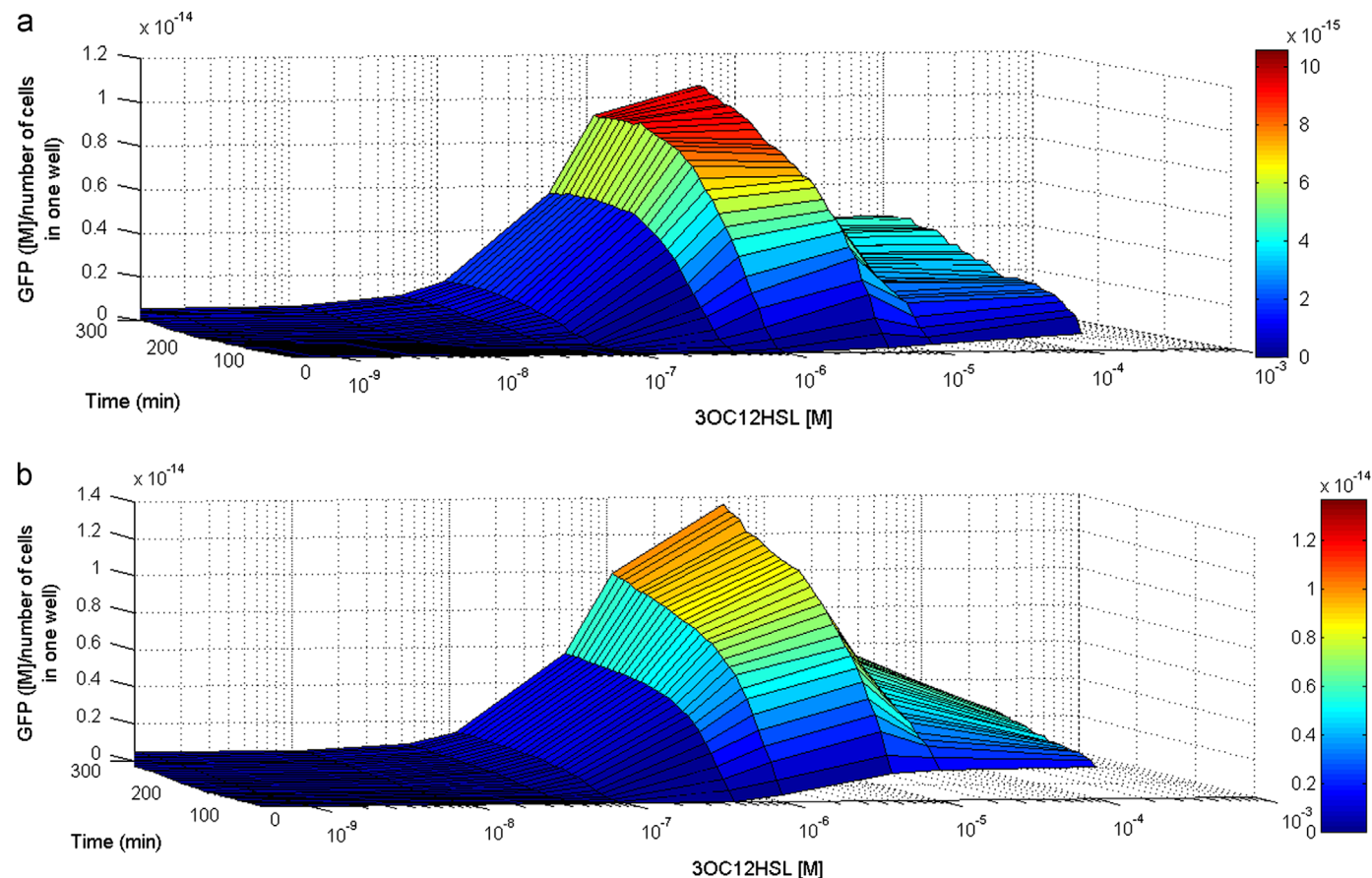


Fig. 2. Characterization results of sensing device coupled with GFP reporter. GFP concentration per cell over time at different 3OC<sub>12</sub>HSL inducer concentrations, high GFP production per cell was observed when the input 3OC<sub>12</sub>HSL concentration was in the range of 1E–6. (A) First experiment set was used to derive parameters of the model. (B) Second set was used for modeling validation.

translation sites on a LasR mRNA we also considered the distance between each ribosome on the mRNA and the length of LasR mRNA. Based on our doubling time which is 60 min, the required distance between each ribosome is 85 nucleotides. As the length of mRNA<sub>LasR</sub> is 723 nucleotides, the number of active translation site on a mRNA<sub>LasR</sub> is 8.5 (Bremer, 1996). Therefore,  $k_2$  was calculated to be  $0.595 \text{ s}^{-1}$  or  $35.7 \text{ min}^{-1}$ .

To estimate the parameters in Eqs. (6.1) and (6.2),  $1/T$  and  $GFP_{max}$  at different concentrations of AHL were first derived by fitting Eq. (10) to the first set of experimental data (summarized in Table 3). Overall, the  $R^2$  of the fittings related to AHL concentration from  $1\text{E}-8$  to  $1\text{E}-6 \text{ M}$  were more than 0.9, showing high correlation between experimental data and fitted graphs.

Using the  $1/T$  and  $GFP_{max}$  derived, Eqs. (6.1) and (6.2) were fitted to the curve  $1/T$  versus AHL concentrations and  $GFP_{max}$  versus AHL concentrations, respectively. Table 4 shows the parameters that were derived for Eqs. (6.1) and (6.2). The experimental results show

that both  $GFP_{max}$  and  $1/T$  increases in a hill equation like manner as the concentration of AHL increases.  $GFP_{max}$  and  $1/T$  correspond to the steady state and dynamic performance of the quorum sensing device to different AHL concentrations, respectively. This implies that the steady state amount of GFP and the rate of GFP production increase when AHL concentration increases from  $1\text{E}-8$  to  $1\text{E}-6 \text{ M}$  and reaches a plateau after  $1\text{E}-6 \text{ M}$ .

### 3.3. Sensitivity analysis

There are a number of parameters in the model developed. To determine the parameters which have large effect on the model in terms of steady state GFP produced and time for GFP production to reach steady state, sensitivity analysis was performed. Fig. 3a and b show the sensitivity analysis results based on changes in  $GFP_{max}$  and time for GFP production to reach steady state, respectively.

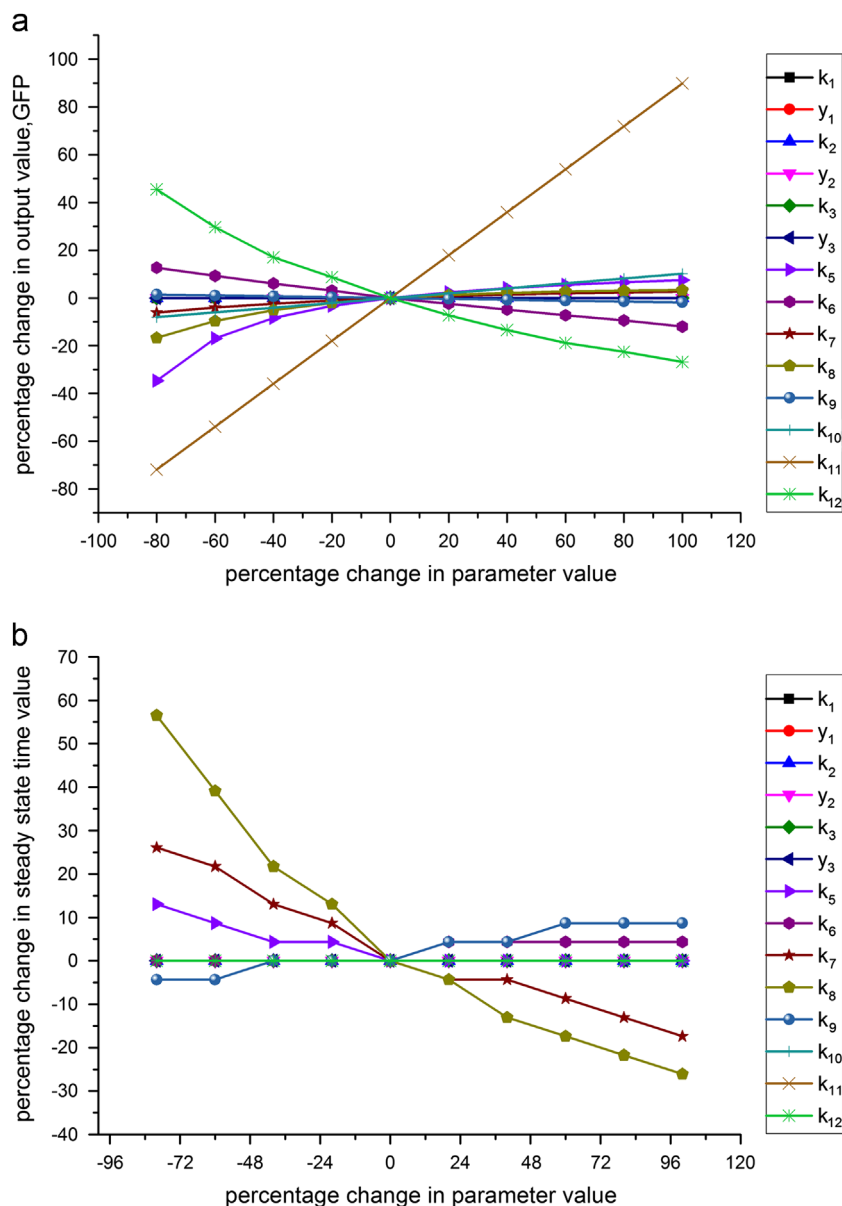


**Fig. 3.** Sensitivity analysis: (A) sensitivity analysis on all the parameters for Eqs. (1)–(6), ranging from  $-80\%$  to  $+100\%$  of original value, changes in output taken at 300 min and with inducer concentration of  $5\text{E}-7 \text{ M}$ . It was observed that  $k_{11}$  (switch point) and  $k_{12}$  (maximum output) of Eq. (6.2), are the most sensitive parameters. (B) Sensitivity analysis on all the parameters for Eqs. (1)–(6), ranging from  $-80\%$  to  $+100\%$  of original value, changes in time to reach steady state. It was observed that  $k_8$  ( $1/k_8$  represents the minimum time to reach 63.2% of the final output) and  $k_7$  ( $1/k_7$  represents the time to reach 63.2% of the final output when there is no induction) of Eq. (6.1) are the most sensitive parameters to define the time which our system needs to reach steady state condition.

For sensitivity analysis of changes in  $GFP_{max}$ , the simulation results (Fig. 3a) show that  $k_{11}$  (maximum output) and  $k_{12}$  (switch point) of Eq. (6.2) were the two most sensitive parameters that greatly affect the final output of the quorum sensing device.

For sensitivity analysis of changes in time to reach steady state, Fig. 3b shows that  $k_8$  ( $1/k_8$  represents the minimum time to reach 63.2% of the final output) and  $k_7$  ( $1/k_7$  represents the time to reach 63.2% of the final output when there is no induction) of Eq. (6.1) were the two most sensitive parameters. These two parameters greatly affect the time at which the system reaches steady state. The other parameters are relatively insensitive mainly because reactions 1–5 are very fast reactions as compared to reaction 6. The sensitivity of the parameters is independent of AHL concentrations, except

$k_{11}$  and  $k_{12}$ . An observation made is that  $k_{11}$  (maximum output) becomes more sensitive while  $k_{12}$  (switch point) becomes less sensitive at higher AHL concentration.

### 3.4. Model validation

To verify the accuracy of our proposed model, an independent second set of experimental data was obtained and compared with the simulation results computed by our model. Fig. 4a and b shows the dynamic and steady state comparison between the experimental and simulated data. For the dynamic comparison (Fig. 4a), at all three different inducer concentrations (low, medium and high), the simulated result matched well with the

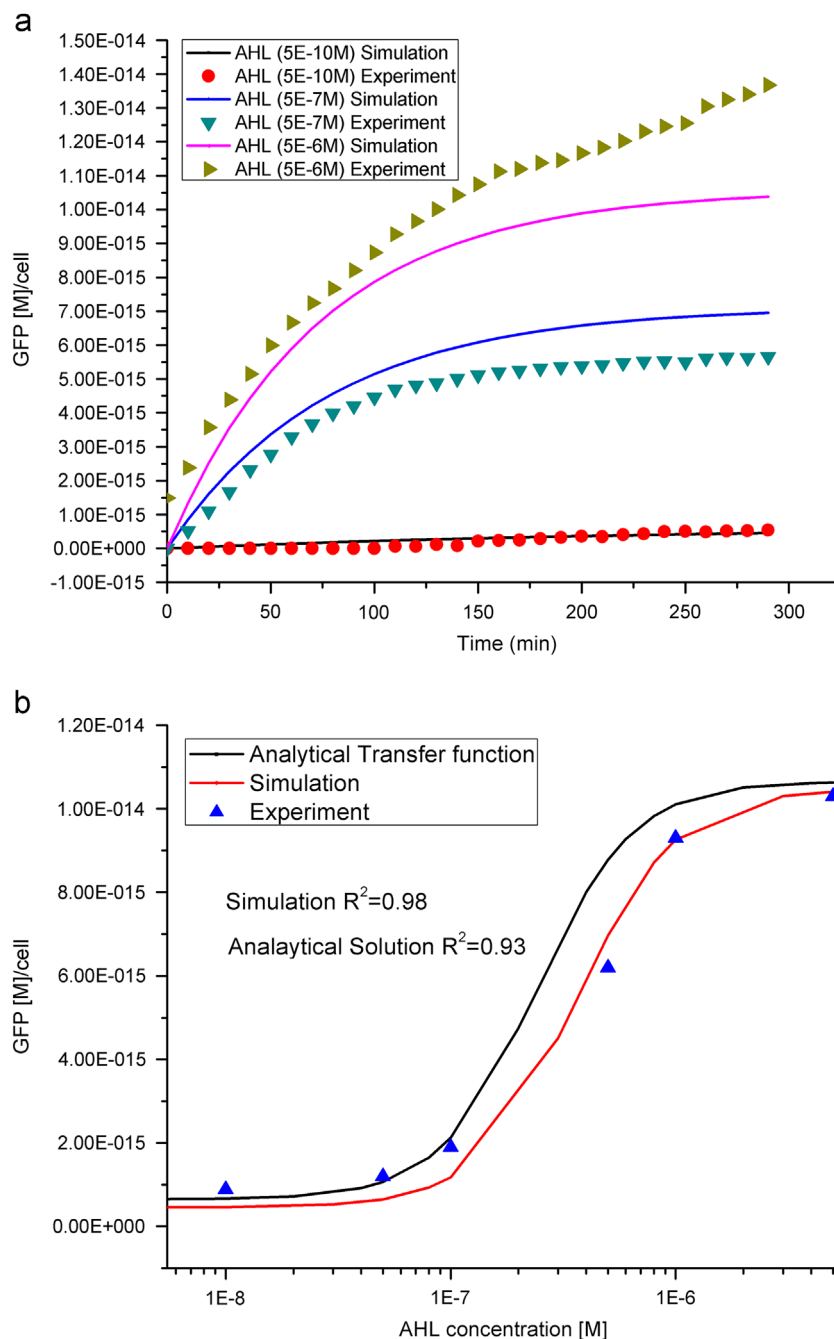


**Fig. 4.** Modeling validation: (A) validation of dynamic performance for three different inducer concentrations, (low, medium and high input). It was observed from the data that the dynamic performance of the quorum sensing device simulated by the proposed model matched well with the experimental data. (B) Steady state modeling validation, based on the output taken at 300 min, it is verified that the maximum GFP production for different input concentrations can be reproduced by the simulation results as well as the analytical solution of the ODEs.

experimental data. The close matching of simulated and the experimental data shows that our proposed model is able to simulate the dynamic performance of quorum sensing system using the derived parameters. Fig. 4b shows that for the steady state performance, both simulation results and analytical transfer function matched well with the experimental result with  $R^2=0.98$  and  $R^2=0.93$  respectively. Hence, it is verified that the maximum GFP production can be reproduced using the proposed model. Eq. (11) shows the analytical transfer function

$$[GFP] = 6.5E-16 + \frac{1E-14[AHL]^2}{2.4E-7^2 + [AHL]^2} \quad (11)$$

### 3.5. Model format and annotation

The model is stored using SBML format and it follows both MIRIAM and MIASE requirements (Novere et al., 2005; Waltemath et al., 2011). One of the essential elements to create a standard biological model is to encode it in a machine-readable and searchable format such as SBML (Endler et al., 2009; Hucka et al., 2003) and CellML (Cuellar et al., 2003). SBML was chosen in our study mainly because it has been more widely used, although saving in other formats is possible. These bioparts description languages enable the description of qualitative and quantitative characteristics of biochemical networks as well as definition of modules and hierarchies between them (Rouilly et al., 2007). In these languages, all elements can be annotated and commented in both human-readable and machine-interpretable forms, allowing extensive documentation and external references to be directly included in the model file. It allows for easier sharing of quantitative models among the community which is making them available. That is why a set of rules in a standardized approach (MIRIAM) has been proposed for the curation of model collection and encoding. Table 5 shows all the species and biological reactions in our developed model which are fully annotated following MIRIAM. This enables the species and biological reactions to be searchable as they have unique identity.

Although MIRIAM promotes the communication and reusability of quantitative biochemical models, it is not adequate for efficient reuse of models in a quantitative setting. It is essential to include the core information required to perform the simulation of quantitative models, as described in MIASE (Waltemath et al., 2011). In this study, our proposed model adhered to the MIASE requirements so as to improve the reusability of the model, which is important to extend the usefulness of the model for synthetic biology design. One of the key points in presenting a simulation experiment is the initial/boundary conditions of different components in the system. Table 6 shows all the species in our model with their corresponding initial concentration.

**Table 5**  
Annotation of species and reactions following MIRIAM.

Species	Database	ID
mRNA <sub>LasR</sub>	CHEBI	CHEBI:33699
LasR	UniProt	P25084
3OC <sub>12</sub> HSL	CHEBI	CHEBI:56080
LasR-AHL	Gene ontology	GO:0005667
pLuxR	PubMed	1987152
A.pluxR	Gene ontology	GO:0000428
GFP	UnitProt	P42212
Eq. (1)	Gene ontology	GO:0009299
Eq. (2)	Gene ontology	GO:0006412 and GO:0030163
Eq. (3)	Gene ontology	GO:0008134
Eq. (4)	Gene ontology and pubmed	GO: 0008134 and PMID: 15623555
Eq. (5)	Gene ontology	GO:0010843
Eq. (6)	Gene ontology	GO: 0006412

**Table 6**  
Initial concentration of specie following MIASE.

Species	Initial concentration
pTet-LasR	1E–5 M
mRNA <sub>LasR</sub>	1E–6 M
LasR	1E–6 M
3OC <sub>12</sub> HSL	Range from 0 to 5E–6 M
LasR-AHL	0 M
pLuxR	1E–5 M
A.pluxR	0 M
GFP	0 M/cell

## 4. Discussion

To facilitate the design of complex systems using the bottom-up approach, we need the help of computational tools. These tools can help us to understand the system behavior *in silico* first before proceeding to the labs to carry out the actual construction but there are challenges in using CAD tools. One of the challenges is that these tools need information about the parts. We developed a model which can describe the kinetics of a quorum sensing device as well as its dynamic and steady state performance. The quorum sensing device has been used in an earlier study as part of a larger biological system which is able to sense and kill *P. aeruginosa* (Saeidi et al., 2011a, 2011b). Our model is in standard SBML format and it complies to both MIRIAM and MIASE requirements. Our model provides detailed annotated reactions involved during the gene expression of the quorum sensing device under certain conditions. One could imagine having a datasheet for the model similar to that proposed by Canton et al. for biological parts. The model datasheet, together with the model will complement the datasheet of biological parts, facilitating future use of the biological parts.

All the parameters related to Eqs. (1)–(5) were derived from literature. Parameters of Eq. (6) with sub-eqs. (6.1) and (6.2) which were derived based on experimental data fitting related to  $1/T$  and  $GFP_{max}$ , respectively. Our experimental findings show that  $1/T$  which represents the time for the system to reach 63.2% of the final output follows a hill equation manner. The experimental results show that the rate at which the device reaches to 63.2% of the final output increases sharply at AHL concentration of  $9.74E-8$  M (switch point) and reaches a max rate at AHL concentration of  $5.0E-6$  M. The  $GFP_{max}$  produced also follows similar trend, the switch point for Eq. (6.2) occurs at AHL concentration of  $2.4E-7$  M and maximum amount of  $GFP_{max}$  is produced at AHL concentration of  $5.0E-6$  M. In our study, data fittings of Eqs. (6.1) and (6.2) were done based on three assumptions. (i) Both Hill coefficients (e.g.  $n_1$  and  $n_2$ ) are assumed to be two because quorum sensing transcription factors generally dimerize prior to binding to the promoter region as reported by earlier studies (Fuqua et al., 2001; Nasser and Reverchon, 2007; Zhu and Winans, 2001). By considering this assumption, the curve was able to fit well with the experimental results. (ii) We considered that the concentration of active complex A.pluxR is equal to the input AHL concentration. Because in our construct LasR is constitutively being expressed under the control of pTetR promoter, we assumed that LasR amount is an excess when we introduced AHL. Furthermore, we are using PSB1A2 which is a high copy number plasmid (100–300 per cell). Taken together, considering pluxR in excess is a reasonable assumption. Because LasR and pLuxR are in excess, LasR-AHL and A.pluxR amount will mainly depend on the input AHL concentration. (iii) The model is simulated deterministically which does not include the randomness that exists in natural systems, while stochastic model do. Nonetheless, the simulation results show that the model is able to reproduce the steady state and dynamic performance of the quorum sensing device under these assumptions.



Sensitivity analysis was performed to study the effect of individual parameter on the final output of the device and the time for the output to reach steady state. The simulation results from sensitivity assay shows that the most significant parameters are in Eq. (6).  $k_{11}$  and  $k_{12}$  of Eq. (6.2) were the most sensitive parameters in term of output amount while  $k_8$  and  $k_7$  of Eq. (6.1) had the most significant effect on the time to reach steady state condition. In Eq. (6.2),  $k_{11}$  is the most sensitive parameter in which a change in  $k_{11}$  will cause a similar percentage change in the final output, whereas a 100% change in  $k_{12}$  will cause about 30% change in the final output. On the other hand, in Eq. (6.1), a change in  $k_8$  will cause a similar change in the time to reach steady state, while a 100% change in  $k_7$  will cause about 20% change in the time to reach steady state point. The other parameters in Eqs. (1)–(5) which were derived from literature have shown negligible sensitivity on the output amount and the time to reach steady state. Therefore our approach to use literature for these data derivation is reasonable. Although the sensitivity analysis shows that only these 4 parameters are sensitive to the overall device performance, we embedded the reactions into the model in order to facilitate future merging of the models of different parts/devices to create the model of the desired composed system, in a similar manner described by semanticSBML (Krause et al., 2010) and OREMPdb (Umeton et al., 2012). When there is a large number of well-validated models of biological parts in databases like BioModels.net, researchers working on new systems could search and import relevant models to be used in their own system modeling. This will enable more efficient building of models.

Although our proposed model was able to characterize the steady state and dynamic performance of the sensing device under similar conditions, the model can be further improved to take account different conditions such as different growing medium, different host strains, different plasmids etc. One possible approach is to study and establish the relationship of the parameters in the model with respect to a change in the conditions, for example changing the medium. This relationship can then be incorporated into the model to enable the model to capture a change in the medium.

## 5. Conclusions

The simulation results show that our proposed model agrees well with the experimental results. The accuracy of our proposed model was validated by carrying out dynamic and static modeling verification. Consequently, the model developed could be used to predict the GFP production under that current set of experimental conditions (e.g. temperature is fixed at 37 °C). The model could be extended in the future to capture characteristics when these experimental conditions vary so that the model can be more versatile. The model could provide useful information about the biological parts for future CAD applications for synthetic biology design.

## Acknowledgments

The authors would like to thank Dr. Forbes Dewey from MIT for his valuable suggestions and comments about the project. This research was supported by the National Medical Research Council of Singapore (CBRG11nov109) and the National Research Foundation of Singapore (NRF-CRP5-2009-03).

## References

- Anderson, J., Dueber, J., Leguia, M., Wu, G., Goler, J., Arkin, A., et al., 2010. BglBricks: A flexible standard for biological part assembly. *J. Biol. Eng.* 4, 1–12.
- Basu, S., Gerchman, Y., Collins, C.H., Arnold, F.H., Weiss, R., 2005. A synthetic multicellular system for programmed pattern formation. *Nature* 434, 1130–1134.
- Bremer, H., Dennis, P.P., 1996. Modulation of chemical composition and other parameters of the cell by growth rate. American Society for Microbiology, Washington, D.C.
- Canton, B.L., Anna, Endy Drew, 2008. Refinement and standardization of synthetic biological parts and devices. *Nat. Biotech.* 26, 787–793.
- Charlton, T.S., de Nys, R., Netting, A., Kumar, N., Hentzer, M., Givskov, M., et al., 2000. A novel and sensitive method for the quantification of N-3-oxoacyl homoserine lactones using gas chromatography-mass spectrometry: application to a model bacterial biofilm. *Environ. Microbiol.* 2, 530–541.
- Cuellar, A.A., Lloyd, C.M., Nielsen, P.F., Bullivant, D.P., Nickerson, D.P., Hunter, P.J., 2003. An Overview of CellML 1.1, a biological model description language. *Simulation* 79, 740–747.
- Elowitz, M.B., Leibler, S., 2000. A synthetic oscillatory network of transcriptional regulators. *Nature* 403, 335–338.
- Endler, L., Rodriguez, N., Juty, N., Chelliah, V., Laibe, C., Li, C., et al., 2009. Designing and encoding models for synthetic biology. *J. R. Soc. Interface* 6 (Suppl 4), S405–417.
- Endy, D., 2005. Foundations for engineering biology. *Nature* 438, 449–453.
- Fagerlind, M.G., Nilsson, P., Harlén, M., Karlsson, S., Rice, S.A., Kjelleberg, S., 2005. Modeling the effect of acylated homoserine lactone antagonists in *Pseudomonas aeruginosa*. *Biosystems* 80, 201–213.
- Funahashi, A., Matsuoka, Y., Jouraku, A., Morohashi, M., Kikuchi, N., Kitano, H., 2008. CellDesigner 3.5: A versatile modeling tool for biochemical networks. *IEEE*, 1254–1265.
- Funahashi, A., Morohashi, M., Kitano, H., Tanimura, N., 2003. CellDesigner: a process diagram editor for gene-regulatory and biochemical networks. *BIOILICO* 1, 159–162.
- Fuqua, C., Parsek, M.R., Greenberg, E.P., 2001. Regulation of gene expression by cell-to-cell communication: acyl-homoserine lactone quorum sensing. *Annu. Rev. Genet.* 35, 439–468.
- Hooshanghi, S., Thiberge, S., Weiss, R., 2005. Ultrasensitivity and noise propagation in a synthetic transcriptional cascade. *Proc. Nat. Acad. Sci. USA* 102, 3581–3586.
- Hucka, M., Finney, A., Sauro, H.M., Bolouri, H., Doyle, J.C., Kitano, H., et al., 2003. The systems biology markup language (SBML): a medium for representation and exchange of biochemical network models. *Bioinformatics* 19, 524–531.
- Kaufmann, G.F., Sartorio, R., Lee, S.-H., Rogers, C.J., Meijler, M.M., Moss, J.A., et al., 2005. Revisiting quorum sensing: Discovery of additional chemical and biological functions for 3-oxo-N-acylhomoserine lactones. *Proc. Nat. Acad. Sci. USA* 102, 309–314.
- Krause, F., Uhlendorf, J., Lubitz, T., Schulz, M., Klipp, E., Liebermeister, W., 2010. Annotation and merging of SBML models with semanticSBML. *Bioinformatics* 26, 421–422.
- Ling, H., Saeidi, N., Haji Rasouliha, B., Chang, M., 2010. A predicted S-type pyocin shows a bactericidal activity against clinical *Pseudomonas aeruginosa* isolates through membrane damage. *FEBS Letter* 3354–3358.
- Nasser, W., Reverchon, S., 2007. New insights into the regulatory mechanisms of the LuxR family of quorum sensing regulators. *Anal. Bioanal. Chem.* 387, 381.
- Novere, N.L., Finney, A., Hucka, M., Bhalla, U.S., Campagne, F., Collado-Vides, J., et al., 2005. Minimum information requested in the annotation of biochemical models (MIRIAM). *Nat. Biotech.* 23, 1509–1515.
- Pearson, J.P., Passador, L., Iglewski, B.H., Greenberg, E.P., 1995. A second N-acylhomoserine lactone signal produced by *Pseudomonas aeruginosa*. *Proc. Natl. Acad. Sci. USA* 92, 1490–1494.
- Ro, D.K., Paradise, E.M., Ouellet, M., Fisher, K.J., Newman, K.L., Ndungu, J.M., et al., 2006. Production of the antimalarial drug precursor artemisinic acid in engineered yeast. *Nature* 440, 940–943.
- Rouilly, V., Canton, B., Nielsen, P., Kitney, R., 2007. Registry of BioBricks models using CellML. *BMC Syst. Biol.* 1, 1–2.
- Saeidi, N.W.C., Lo, T., Nguyen, H.X., Ling, H., Leong, S.S.J., Poh, C.L., et al., 2011a. Engineering microbes to sense and eradicate *Pseudomonas aeruginosa*, a human pathogen. *Mol. Syst. Biol.*
- Saeidi, N., Wong, C.K., Lo, T.-M., Nguyen, H.X., Ling, H., Leong, S.S.J., et al., 2011b. Engineering microbes to sense and eradicate *Pseudomonas aeruginosa*, a human pathogen. *Mol. Syst. Biol.*, 7.
- Shetty, R., Knight T, E.D., 2008. Engineering BioBrick vectors from BioBrick parts. *J. Bio. Eng.* 2, 5–6.
- Sinha, J., Reyes, S.J., Gallivan, J.P., 2010. Reprogramming bacteria to seek and destroy an herbicide. *Nat. Chem. Biol.* 6, 464–470.
- Steen, E.J., Kang, Y., Bokinsky, G., Hu, Z., Schirmer, A., McClure, A., et al., 2010. Microbial production of fatty-acid-derived fuels and chemicals from plant biomass. *Nature* 463, 559–562.
- Umeton, R., Nicosia, G., Dewey, C.F., 2012. OREMPdb: a semantic dictionary of computational pathway models. *BMC Bioinformatics* 13, S6.
- Vogel, U., Jensen, K.F., 1994. The RNA chain elongation rate in *Escherichia coli* depends on the growth rate. *J. Bacteriol.* 176, 2807–2813.
- Waltemath, D., Adams, R., Beard, D.A., Bergmann, F.T., Bhalla, U.S., Britten, R., et al., 2011. Minimum information about a simulation experiment (MIASE). *PLoS Comput. Biol.* 7, e1001122.
- Zhu, J., Winans, S.C., 2001. The quorum-sensing transcriptional regulator TraR requires its cognate signaling ligand for protein folding, protease resistance, and dimerization. *Proc. Natl. Acad. Sci. USA* 98, 1507–1512.